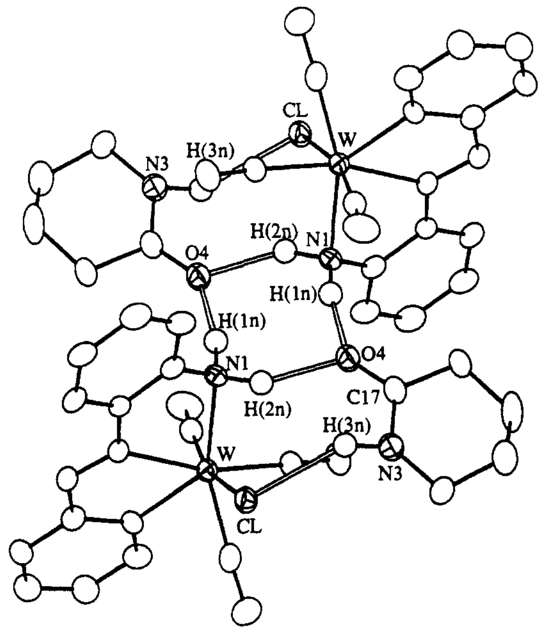

Figure 1. ORTEP representation of **3**. Hydrogen bonds are indicated by open bonds, and the disordered THF solvate which is not involved in the hydrogen bonding is omitted.

^1H NMR shifts for a titration of **3**,[11] which contains a chloride bound to tungsten, with val were similar although the binding constant (K_3 = 1.3 ± 0.5 M^{-1}) is smaller. The more electronegative fluoride appears to be a better hydrogen bond acceptor than chloride when coordinated to tungsten(II).

The solution NMR data for the interaction of **1**–**3** with val suggest the chelating structure depicted in Scheme I. Solid-state structural studies of **3** provide support for this formulation.[12] Like the tungsten fluoride **1**, the chloride **3** crystallizes as a head-to-tail dimer. Relevant metrical parameters are given in Scheme I; the NH···Cl distance is consistent with hydrogen bonding in the solid state.[13] The Et_2O solvate is tightly bound to H(1n).

Cocrystallization of **3**·Et_2O with 5 equiv of val in THF by vapor diffusion of Et_2O affords single crystals of the adduct **4** as illustrated in Figure 1.[14] Dimers of **4** related by a center of inversion generate the tetrameric structure. Hydrogen bonding between **3** and val is clearly evident as depicted in Scheme I (lower half). Note that the NH(3n)···Cl distance in **4** is shorter than the related interval in the homomolecular dimer **3**. This suggests that stronger hydrogen-bonding interactions exist in the heterodimer **4** relative to the parent compound **3**. Solid-state IR spectra show that the amide carbonyl stretching frequency of val is reduced by 42 cm^{-1} upon complex formation; the NH bands broaden and shift to lower frequency (ν_{NH} = 3278 (m), 3235 (m), 3125 (m) cm^{-1}) compared to free val.[7]

Preliminary experiments show that **1** also interacts with protected nucleosides in nonaqueous solution. The binding constant for 2′,3′-*O*-isopropylidene-5′-*O*-acetyl uridine[15] in acetone is 3.6 M^{-1} at 25 °C. Although the strength of the binding is modest, these studies show that transition-metal complexes possessing *cis*-amino halide ligands can act as ditopic molecular receptors for biologically relevant molecules. This property should be general and most evident for coordination complexes containing fluoride. Elimination of HF[16] from hydrogen-bonded complexes such as these may enable a covalent host–guest linkage to be formed. We are continuing to investigate the chemistry of this new class of receptors.

Acknowledgment. We thank Professor D. A. Dougherty (California Institute of Technology) for a copy of the NMRFIT program, Professor C. D. Poulter for helpful discussions, and the referees for cogent comments. T.G.R. is the recipient of a Distinguished New Faculty Grant from the Camille and Henry Dreyfus Foundation Inc. We are grateful for support from the donors of the Petroleum Research Fund, administered by the American Chemical Society, and the University of Utah Research Committee. High field NMR spectrometers employed in this work were obtained through departmental grants from the National Science Foundation.

Supplementary Material Available: Titration data for complexes **1**–**3** and full crystallographic data for **3**·Et_2O and **4**·THF including tables of bond distances and angles and final positional and thermal parameters (39 pages); a listing of calculated and observed structure factors (39 pages). Ordering information is given on any current masthead page.

---

(11) (a) Preparation of **2** is analogous to our published procedure for **1**:[6a] IR (Nujol mull, cm^{-1}) 3160, 3052 (m, ν_{NH}), 2009, 1934, 1893 (s, ν_{CO}); nonaromatic ^1H NMR δ 9.596 ($^3J_{WH}$ = 7.7 Hz), δ 6.60 (d, J = 11.8 Hz), δ 6.15 (d, J = 11.8 Hz). Anal for **2**·Et_2O. Calcd $C_{20}H_{21}N_2ClO_4W$: C, 41.95; H, 3.70; N, 4.89. Found: C, 42.05; H, 3.55; N, 5.02. (b) Binding constant determined by averaging K_3 for each proton.

(12) Crystal data for **2**·Et_2O: $WClO_4N_2C_{20}H_{21}$, red-orange, triclinic, $P\bar{1}$, a = 10.172 (3) Å, b = 10.524 (4) Å, c = 11.117 (4) Å, α = 115.52 (2)°, β = 101.24 (3)°, γ = 84.04 (3)°, V = 1053.2 Å^3, Z = 2, Mo Kα. Of 3751 reflections collected at ambient temperature (Syntex P1, 2° < 2θ < 49°) 3305 were unique of which 3118 had $I > 3\sigma(I)$ and were used in the solution and refinement (SDP PLUS Software). Final refinement included all non-hydrogen atoms as anisotropic and hydrogen atoms as idealized isotropic contributions. All hydrogens were located on a difference map but not refined. For 253 parameters, R = 0.022 and R_w = 0.025, GOF = 1.3, and highest peak in the final map of 1.1 e/Å approximately 1.1 Å from W.

(13) (a) Hamilton, W. C.; Ibers, J. A. *Hydrogen Bonding in Solids*; Benjamin: New York, 1968. (b) Bronty, C.; Spinat, P.; Whuler, A. *Acta Crystallogr., Sect. B* **1980**, *36*, 1967. (c) Novak, A. *Struct. Bonding* **1974**, *18*, 177.

(14) (a) Anal for **3**·THF. Calcd $C_{25}H_{28}N_3ClO_5W$: C, 44.83; H, 4.21; N, 6.27. Found: C, 44.73; H, 4.22; N, 6.27. (b) Crystal data for **3**·THF: $WClO_5N_3C_{25}H_{28}$, red-orange, monoclinic, $C2/c$, a = 19.939 (5) Å, b = 14.025 (4) Å, c = 19.411 (4) Å, β = 99.44 (2)°, V = 5354.5 Å^3, Z = 8, Mo Kα. Of 4319 reflections collected at ambient temperature (Syntex P1, 2° < 2θ < 48°) 4049 were unique of which 2750 had $I > 3\sigma(I)$ and were used in the solution and refinement (SDP PLUS Software). Final refinement included all non-hydrogen atoms as anisotropic and hydrogen atoms as idealized isotropic contributions. H(1n), H(2n), and H(3n) were located on a difference map, and remaining hydrogens were placed in calculated positions but not refined. For 271 parameters, R = 0.054 and R_w = 0.074, GOF = 1.7, and highest peak in the final map of 1.3 e/Å^3 approximately 0.80 Å from W.

(15) (a) Iwahashi, H.; Kyogoku, Y. *J. Am. Chem. Soc.* **1977**, *99*, 7761. (b) Reuben, J. *J. Am. Chem. Soc.* **1987**, *109*, 316. (c) Gmeiner, W. H.; Poulter, C. D. *J. Am. Chem. Soc.*, in press.

(16) (a) Basolo, F.; Matoush, W. R.; Pearson, R. G. *J. Am. Chem. Soc.* **1956**, *78*, 4833.

Photochemical Activation of CO_2. Transient Absorbance Kinetic Studies of the Addition of CO_2 to a Metal-to-Bridging Ligand Charge-Transfer State of a Binuclear Ni(0) Complex

Frederick R. Lemke, Dru L. DeLaet, Jiali Gao, and
Clifford P. Kubiak*,[1]

Department of Chemistry, Purdue University
West Lafayette, Indiana 47907

Received June 13, 1988

We report the photochemical activation of CO_2 by a ligand-centered charge-transfer excited state of a binuclear Ni(0) complex. The activation and reduction of carbon dioxide are areas of considerable interest and potential importance for artificially recycling the products of combustion and respiration.[2-16] Among

---

[1] Research Fellow of the Alfred P. Sloan Foundation, 1987–1989.

(2) Eisenberg, R.; Hendriksen, D. E. *Adv. Catal.* **1979**, *28*, 79.

(3) Palmer, D. A.; van Eldik, R. *Chem. Rev.* **1983**, *83*, 651.

(4) Darensbourg, D. J.; Kudaroski, R. A. *Adv. Organomet. Chem.* **1983**, *22*, 129.

(5) Inoue, S.; Koinuma, H.; *Rev. Inorg. Chem.* **1984**, *6*, 291.

(6) Lundquist, E. G.; Huffman, J. C.; Caulton, K. G. *J. Am. Chem. Soc.* **1986**, *108*, 8309.

(7) Lee, G. R.; Cooper, N. J. *Organometallics* **1985**, *4*, 1467.

(8) DeLaet, D. L.; del Rosario, R.; Fanwick, P. E.; Kubiak, C. P. *J. Am. Chem. Soc.* **1987**, *109*, 754.

Scheme I. Photochemistry of $Ni_2(\mu\text{-}CNMe)(CNMe)_2(dppm)_2$, **1**, with CO_2 and PhCl

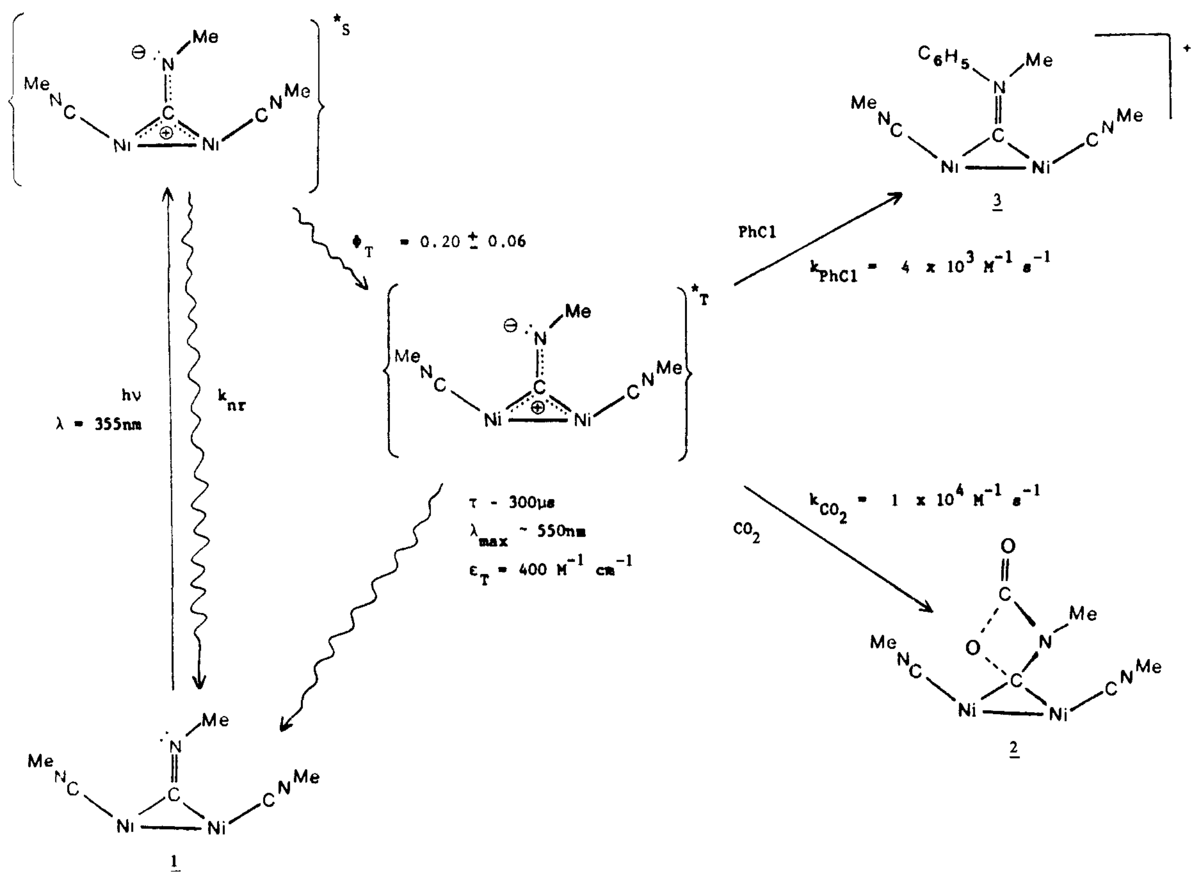

the various chemical,[2-8] electrochemical,[8-12] and photochemical[13-16] approaches to CO_2 activation by transition-metal complexes, photochemical methods have received the least attention. Excited states of transition-metal complexes are generally dissociative with respect to metal–ligand or metal–metal bonding; and CO_2 is not a common ligand in either ground or excited state complexes. The chemistry and electrochemistry of the binuclear nickel (0) complex $Ni_2(\mu\text{-}CNMe)(CNMe)_2(dppm)_2$ (**1**) (dppm = bis(diphenylphosphino)methane) with CO_2 were recently reported.[8] A photochemical reaction of **1** with CO_2 also was noted.[13] We now describe our studies of the spectroscopy and reactivity of the excited state involved in the photochemical reaction of **1** with CO_2.

Photolysis of THF solutions of **1** in the presence of CO_2 (1 atm) leads to the formation of a CO_2 cycloadduct with the μ-CNMe ligand. The product of the photochemical reaction, $Ni_2(\mu\text{-}\overline{CN(Me)C(O)O})(CNMe)_2(dppm)_2$, **2**, is formed with an overall quantum yield, $\Phi_{355} = 0.05$, eq 1, and is identical with the product of the thermal reaction of **1** with liquid CO_2 at 25 °C, described earlier.[8] There is no evidence for a dark reaction of **1** with CO_2 at pressures 3 atm or less. The photochemical reaction of **1** with CO_2 at 1 atm is the first example of a bimolecular association of CO_2 to an excited state of a transition-metal complex. We note that **1** does not emit, even as a crystalline solid at 77 K. Therefore transient absorbance kinetic studies were undertaken to probe this unusual photochemistry.

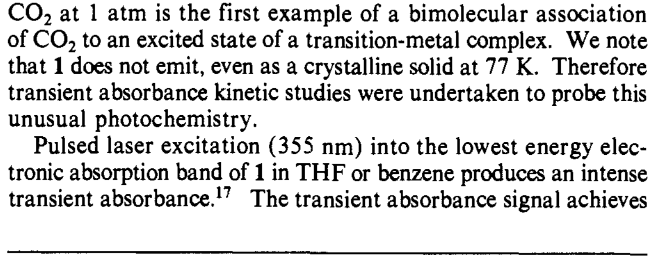

(1)

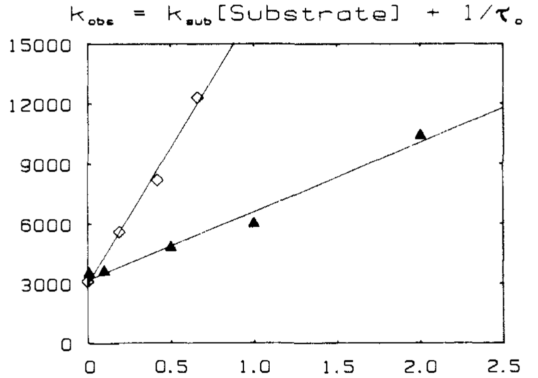

Figure 1. Plots of $k_{obsd} = 1/\tau$, the rate of disappearance of Nd-YAG laser ($3\nu_0$, 355 nm) induced transient absorbance of $Ni_2(\mu\text{-}CNMe)(CNMe)_2(dppm)_2$, **1**, at 550 nm, versus $[CO_2]$ (◇) and [PhCl] (▲).

Pulsed laser excitation (355 nm) into the lowest energy electronic absorption band of **1** in THF or benzene produces an intense transient absorbance.[17] The transient absorbance signal achieves

---

(9) Wu, J.; Fanwick, P. E.; Kubiak, C. P. *Organometallics* **1987**, *6*, 1805.

(10) Fisher, B. J.; Eisenberg, R. *J. Am. Chem. Soc.* **1980**, *102*, 7361.

(11) Bruce, M. R. M.; Megehee, E.; Sullivan, B. P.; Thorp, H.; O'Toole, T. R.; Downard, A.; Meyer, T. J. *Organometallics* **1988**, *7*, 238 and references therein.

(12) Frese, K. W.; Summers, D. P.; Cinibulk, M. *J. Electrochem. Soc.* **1988**, *135*, 264.

(13) DeLaet, D. L.; Fanwick, P. E.; Kubiak, C. P. *J. Chem. Soc., Chem. Commun.* **1987**, 1412.

(14) (a) Hawecker, J.; Lehn, J.-M.; Zeissel, R. *J. Chem. Soc., Chem. Commun.* **1983**, 536. (b) Lehn, J.-M.; Zeissel, R. *Proc. Natl. Acad. Sci. U.S.A.* **1982**, *79*, 701.

(15) Kutal, C.; Corbin, A. J.; Ferraudi, G. *Organometallics* **1987**, *6*, 553.

(16) Belmore, K. A.; Vanderpool, R. A.; Tsai, J.-C.; Khan, M. A.; Nicholas, K. M. *J. Am. Chem. Soc.* **1988**, *110*, 2004.

(17) A complete description and diagramatic layout of the laser flash photolysis system employed in these studies is included as Supplementary Material.

maximum intensity at 550 nm, a region where **1** does not absorb, and decays unimolecularly with $\tau = 300\ \mu s$. The observed signal is assigned to $M_2 \rightarrow \mu$-LCT triplet–triplet absorbance (vide infra). The transient absorbance exhibits partial saturation at high laser powers,[18-20] suggesting that the observed state is formed by a process of limited efficiency from the initial excited state, consistent with $[M_2 \rightarrow \mu\text{-LCT}]^1 \rightarrow [M_2 \rightarrow \mu\text{-LCT}]^3$ conversion. The method of Carmichael and Hug[19] was employed to fit the partial saturation of transient absorbance and obtain the triplet conversion quantum yield, $\Phi_T = 0.2$.

In the presence of CO_2, the rate of disappearance of $[M_2 \rightarrow \mu\text{-LCT}]^3$ absorbance exhibits a first-order dependence on $[CO_2]$. The photochemical kinetics of **1** with CO_2 were examined over the CO_2 pressure range 1–3 atm. Pressures of CO_2 were calibrated against $[CO_2]$ in THF solution by the method of Daniele et al.[21] The lifetime τ of $[M_2 \rightarrow \mu\text{-LCT}]^3$ absorbance exhibits an inverse linear dependence on $[CO_2]$ from which the rate constant for CO_2 addition, $k_{CO_2} = 1 \times 10^4\ M^{-1}\ s^{-1}$, was determined. The $[M_2 \rightarrow \mu\text{-LCT}]^3$ state of **1** is also reactive with respect to the addition of a variety of other reagents. For example PhCl, which is thermally unreactive with **1** when employed as the solvent under reflux, reacts photochemically with the $[M_2 \rightarrow \mu\text{-LCT}]^3$ state with a bimolecular rate constant, $k_{PhCl} = 4 \times 10^3\ M^{-1}\ s^{-1}$, to form the μ-phenyl amino–carbyne complex, $[Ni_2(\mu\text{-CN(Ph)Me})(CNMe)_2(dppm)_2]Cl$, **3**.[22] The dependence of $k_{obsd} = 1/\tau$ for the transient absorbance of **1** versus $[CO_2]$ and [PhCl] is given in Figure 1. The overall photochemical reactivity of **1** with CO_2 and PhCl is presented in Scheme I.

The nature of the lowest energy electronic absorption spectral band of **1** was also assessed by bridging ligand substituent and solvent effects. The electronic absorption spectrum of **1** exhibits an intense, broad band centered at $\lambda_{max} = 345$ nm ($\epsilon = 19\,000\ M^{-1}\ cm^{-1}$) in THF. The series of μ-aryl isocyanide complexes $Ni_2(\mu\text{-L})(CNMe)_2(dppm)_2$, L = CNC_6H_6 (**4**), CN-*p*-C_6H_4Cl (**5**), and CN-*p*-C_6H_4Me (**6**), were prepared by substitution of one of the MeNC ligands of **1**.[23] Within the group of complexes **4–6** values of λ_{max} are quite insensitive to the nature of the para substituent on the aryl group but are shifted to longer wavelengths by 35 nm relative to the μ-methyl isocyanide complex **1** in THF.[23] There are also significant intensity differences between the aryl complexes **4–6** and **1**. The values of ϵ determined for the aryl complexes **4–6** are 20–100% higher than the values for **1** in THF and benzene. The bathochromic shifts and intensity increases resulting from replacement of alkyl substituent with aryl substituents are consistent with metal-to-μ-ligand charge transfer ($M_2 \rightarrow \mu$-LCT).[24] The electronic absorption spectra of the μ-isocyanide complexes **1** and **4–6** also exhibit significant solvent dependence. Hypsochromic shifts as large as 85 nm (THF/MeCN) are observed in more polar solvents. This is consistent with a Frank–Condon destabilized excited state model in which a polar solvent is unable to reorient itself in response to an excited state of polarity markedly different from the ground state. Extended Huckel calculations support the notion of metal-to-bridging ligand charge transfer. In an electronically saturated d^{10}–d^{10} configuration of nickel atoms interacting with unsaturated methyl isocyanide ligands, bridging isocyanide $\pi^*/Ni_2\ d\pi^*$ interactions determine both the HOMO and LUMO.[25] The $\pi^*(\parallel)$ component of the μ-CNMe ligand and highest energy $Ni_2\ d\pi^*$ combination contribute to a HOMO of metal–ligand π-bonding character. The second π^* component ($\perp$) of the μ-CNMe ligand is not disposed by symmetry to interact significantly with the Ni_2 framework and becomes the LUMO. The Huckel description thus predicts a LUMO of essentially pure μ-CNMe π^* character, consistent with the spectroscopic studies described above.

Our results suggest that a long-lived excited state of a binuclear transition-metal complex can be employed to associate with the CO_2 molecule. Previous studies from this laboratory indicate that the association of CO_2 with **1** results in the activation of CO_2 toward oxygen atom transfer reactions.[8,13] Continued studies of the photochemical activation and reduction of CO_2 are presently underway.

Acknowledgment. We are extremely grateful to Professor George McLendon (Rochester), Professors Dave McMillin and Ed Grant (Purdue), and Dr. Jay Winkler (Brookhaven) for suggestions and helpful discussions, Profesor William Jorgensen (Purdue) for assistance and support with extended Huckel calculations, and NSF (CHE-8707963) for support.

Supplementary Material Available: Description and diagrammatic layout of laser flash photolysis system; preparative details, IR, UV–vis, and $^{31}P\{^1H\}$ NMR spectroscopic data for **4**, **5**, and **6**; transient absorbance versus laser power data; and details of the determination of triplet conversion quantum yield (5 pages). Ordering information is given on any current masthead page.

---

(18) Transient absorbance versus laser power data and details of the determination of the triplet conversion quantum yield, Φ_T, are included as Supplementary Material.

(19) (a) Carmichael, I.; Hug, G. L. *J. Phys. Chem.* **1985**, *89*, 4036. (b) Hug, G. L.; Carmichael, I. *J. Photochem.* **1985**, *31*, 179.

(20) Murasecco-Suardi, P.; Gassmann, E.; Braun, A. M.; Oliveros, E. *Helv. Chim. Acta* **1987**, *70*, 1760.

(21) Daniele, S.; Ugo, P.; Bontempelli, G.; Fiorani, M. *J. Electroanal. Chem.* **1987**, *219*, 259.

(22) Complex **3** was prepared by photolysis (λ = 355 or 366 nm) of a PhCl solution of **1** or, as the corresponding iodide salt, by addition of excess MeI (3 μL, 0.05 mmol) to a THF solution of **4** (0.026 g, 0.025 mmol). Recrystallization from THF/hexanes affords the crystalline solid, yield 90%. $[Ni_2(\mu\text{-}CN(Ph)Me)(CNMe)_2(dppm)_2]Cl$ (*3*): IR (KBr) ν (CN) 2135 s, 1523 m cm^{-1}; $^{31}P\{^1H\}$ NMR δ 20.2 (m); UV–vis (λ_{max} (ϵ)) 550 nm (1600) (THF).

(23) Details of the preparation of complexes **4**, **5**, and **6** and their IR, UV–vis, and $^{31}P\{^1H\}$ data are included as Supplementary Material.

(24) Phifer, C. C.; McMillin, D. R. *Inorg. Chem.* **1986**, *25*, 1329.

(25) All calculations were performed for $Ni_2(\mu\text{-CNH})(CNH)_2(PH_2CH_2PH_2)_2$ with the extended Huckel method. See: Hoffmann, R. J. *J. Chem. Phys.* **1963**, *39*, 1397. the parameters used for nickel were adopted in the present study from earlier work of Hoffmann, see: Hoffmann, D. M.; Hoffmann, R.; Fisel, C. R. *J. Am. Chem. Soc.* **1982**, *104*, 3858.

Transition-State Geometry in Epoxidation by Iron–Oxo Porphyrin at the Compound I Oxidation Level. Epoxidation of Alkenes Catalyzed by a Sterically Hindered (*meso*-Tetrakis(2,6-dibromophenyl)porphinato)iron(III) Chloride

Dražen Ostović and Thomas C. Bruice*

Department of Chemistry
University of California at Santa Barbara
Santa Barbara, California 93106

Received May 9, 1988

Although many studies of iron porphyrin catalyzed epoxidations have appeared in the literature,[1-3] the mechanism of epoxidation remains unresolved. The following mechanisms have been considered: (i) concerted oxygen insertion into the double bond (the oxenoid character of the iron bound oxygen atom supports this

---

(1) *Cytochrome P-450*; *Structure, Mechanism, and Biochemistry*; Ortiz de Montellano, P. R., Ed.; Plenum: New York, 1986.

(2) (a) Watabe, T.; Akamatsu, K. *Biochem. Pharmacol.* **1976**, *23*, 1079. (b) Watabe, T.; Ueno, Y.; Imazumi, J. *Biochem. Pharmacol.* **1971**, *20*, 912. (c) Ortiz de Montellano, P. R.; Mangold, B. L. K.; Wheeler, C.; Kunze, K. L.; Reich, N. O. *J. Biol. Chem.* **1983**, *258*, 4212. (d) Castellino, A. J.; Bruice, T. C. *J. Am. Chem. Soc.* **1988**, *110*, 1313.

(3) (a) Traylor, T. G.; Nakano, T.; Miksztal, A. R.; Dunlap, B. E. *J. Am. Chem. Soc.* **1987**, *109*, 3625. (b) Traylor, T. G.; Nakano, T.; Dunlap, B. E.; Traylor, P.; Dolphin, D. *J. Am. Chem. Soc.* **1986**, *108*, 2782. (c) Traylor, T. G.; Miksztal, A. R. *J. Am. Chem. Soc.* **1987**, *109*, 2770. (d) Castellino, A. J.; Bruice, T. C. *J. Am. Chem. Soc.* **1988**, *110*, 158. (e) Liebler, D. C.; Guengerich, F. P. *Biochemistry* **1983**, *22*, 5482. (f) Mansuy, D.; Leclaire, J.; Fontecave, M.; Momenteau, M. *Biochem. Biophys. Res. Commun.* **1984**, *119*, 319. (g) Groves, J. T.; Subramanian, D. V. *J. Am. Chem. Soc.* **1984**, *106*, 2177.

0002-7863/88/1510-6906$01.50/0